[Research Paper] 대한금속 · 재료학회지 (*Korean J. Met. Mater.*), Vol. 62, No. 4 (2024) pp.292-298
DOI: 10.3365/KJMM.2024.62.4.292

Tuning Dielectric Constant of P3HT by Ultrasound-Induced Aggregation

Byoung-Nam Park*

Department of Materials Science and Engineering Hongik University 72-1, Sangsu-dong, Mapo-gu, Seoul 04066, Republic of Korea.

Abstract: Poly(3-hexylthiophene) (P3HT), a semiconducting polymer, is integral to the development of organic electronic devices. Its optoelectronic properties are significantly influenced by the nature of its intermolecular interactions, predominantly classified as J-type and H-type couplings. This study investigates the effect of sonication on the dielectric properties of P3HT, focusing on the transition from J-type (or less prominent H-type) to H-type intermolecular interactions, accompanied by disorder-order transformation. The research determined that sonication leads to a significant change in the dielectric properties of P3HT by forming distinct ordered regions interspersed within disordered or quasi-ordered areas. Specifically, there is an observable transition from J-type to H-type aggregation, which has profound effects on the material's electronic structure and optoelectronic performance. This transition was confirmed by changes in the absorption and photoluminescence spectra, indicating a more localized electronic character and the formation of non-emissive excitons in the case of H-aggregates. Increased dielectric constant after sonication is attributed to interface polarization, especially the Maxwell-Wagner-Sillars polarization. This effect is likely because new interfaces are created between the ordered regions and disordered/quasi-ordered regions within the P3HT material, where charges can accumulate as a result of disorder-order transformation. Our research contributes to the broader understanding of polymer physics and the development of organic electronic devices by showing how the manipulation of microstructural environments can control material properties.

(Received 12 December, 2023; Accepted 8 January, 2024)

Keywords: dielectric constant, disorder-order transformation, crystallinity, interface polarization

1. INTRODUCTION

In recent advancements in the field of organic semiconductors, the manipulation of the dielectric environment to control the physical and electronic properties of polymeric materials has garnered significant attention[1-3]. This study aims to explore the transformative impact of sonication on the dielectric properties of poly(3-hexylthiophene) (P3HT), a widely studied conjugated polymer known for its promising applications in organic electronics. The critical focus is on the transition of intermolecular interactions from J-type (or less prominent *H*-type) to H-type, induced by the sonication process.

P3HT, characterized by its π-conjugated backbone, exhibits unique electronic and optical properties that are highly sensitive to the nature of its intermolecular interactions[4-7]. Typically, these interactions manifest in two predominant forms: *J*-type and *H*-type coupling[8-13]. *J*-type coupling, often observed in neatly aligned, head-to-tail configurations of polymer chains, is known for its extended conjugation and delocalized excitonic states. Conversely, *H*-type coupling, arising from a face-to-face stacking arrangement, exhibits a more localized electronic character. The balance between these two types of interactions critically influences the charge transport, light absorption, and emission properties of P3HT[14-17].

This investigation utilizes the process of sonication, a technique commonly employed to disperse and de-aggregate materials, to modulate the intermolecular interactions in P3HT. Sonication is hypothesized to impact the polymer's aggregate structure, thereby altering its dielectric constant – a key parameter that governs the electrostatic interactions

- 박병남: 교수
*Corresponding Author: Byoung-Nam Park
[Tel: +82-10-4244-0495, E-mail: metalpbn@gmail.com]

between polymer chains. The aim is to systematically study how sonication-induced changes in the polymer's morphology and chain alignment transition the nature of coupling from J-type (or less prominent *H*-type) to H-type. Such a transition is expected to have profound implications on the electronic structure and, consequently, the optoelectronic performance of P3HT.

Our study reveals that sonication significantly alters the dielectric properties of P3HT, primarily by transitioning from less defined *H*-type to more pronounced *H*-type aggregation. This shift markedly impacts the electronic structure and optoelectronic behavior of the material. Evidence of this transition is apparent in the observed modifications in both absorption and photoluminescence (PL) spectra. Change in the electrical properties after sonication is investigated using field effect transistor (FET) and diode configurations. The electrical property changes induced by sonication were examined using FET and diode configurations to understand their impact. These observations indicate a transition to a stronger interchain interactions, typical of *H*-aggregates, accompanied by the formation of non-emissive excitons characteristic of these aggregates.

Understanding the sonication-driven modulation of dielectric properties and its correlation with the type of intermolecular coupling presents a novel approach to tailor the material properties of organic semiconductors. This study not only contributes to the fundamental understanding of polymer physics but also opens new avenues for optimizing the performance of organic electronic devices, including organic photovoltaics, FETs, and light-emitting diodes.

2. MATERIALS AND METHODS

2.1. Formation of sonicated P3HT film

High-regioregularity P3HT (>96%) was purchased from Sigma Aldrich. P3HT solutions in chloroform, with a concentration set at 10 mg/mL, were prepared for film formation by spin-coating (1500 rpm for 30 seconds) onto a SiO_2 gate dielectric layer of indium-tin oxide (ITO) substrate for fabrication of FET and diode test devices. To promote a more ordered molecular structure within the P3HT films—a factor critical for achieving desirable electronic properties—the solutions were sonicated at a power of 50 W (40 kHz) in a chilled water bath for 10 minutes prior to the spin-coating.

This pre-treatment step is crucial for inducing the desired degree of molecular ordering and interchain interaction, which are pivotal for the film's conductive properties. This sonication resulted in a noticeable change in the solution's appearance, transitioning from a transparent red to a rich, dark wine hue, indicative of increased polymer aggregation. To preserve the quality of the films against oxidative damage, an encapsulation technique was adopted. The films, both pristine and sonicated, were carefully covered with a glass slide. The edges of the glass were sealed using adhesive tape, forming a barrier against environmental factors.

2.2. Fabrication of FETs and Ag/P3HT/ITO diodes and Structural Characterizations

For the investigation of charge transport properties in P3HT, distinct configurations for FETs and diodes were employed. The FET construction involved patterning source and drain electrodes onto a SiO_2 gate dielectric. This patterning was achieved through photolithography, where a 3 nm titanium (Ti) layer was first deposited for enhanced adhesion, followed by an 80 nm gold (Au) layer. The SiO_2 gate dielectric layer (200 nm) was situated atop a heavily doped silicon substrate, which functioned as the gate electrode.

Diode structures were fabricated by applying a P3HT film onto an ITO electrode through a spin-coating process at 1500 rpm for 30 seconds. This method ensured a uniform and thin film of P3HT on the ITO surface. The diode structure was finalized by vacuum-depositing Ag onto the P3HT layer, establishing the necessary contact for effective charge transport. This process is vital for conducting both *I-V* measurements and assessing the frequency-dependent dielectric constant of P3HT.

The electrical measurements were conducted using an HP4145B semiconductor parameter analyzer in an argon-filled glove box to maintain a stable environment. The bottom-contact FET is utilized as an electrical probe to assess the electronic properties of both pristine and sonicated-P3HT films. Specifically, in the linear regime of transistor operation, where the gate voltage (V_G) significantly exceeds the drain voltage (V_D), the drain current (I_D) in the P3HT layers is governed by several factors. These include the

mobility of holes (μ), the capacitance per unit area of the interface (C_i), and the dimensions of the device, namely, the width (Z) and length (L). This relationship can be expressed by the following equation:

$$I_D = \frac{Z}{L}\mu C_i(V_G - V_T)V_D$$

To determine the FET mobility in the linear transport region, we analyze the slope of the linear portion of the I_D-VG curve. This slope is directly proportional to the FET mobility, indicating the efficiency of charge carrier transport within the transistor. By calculating this slope, we can effectively quantify the mobility of holes in the P3HT layers, thereby providing insight into the impact of sonication on the film's electronic properties.

To calculate the dielectric constant, dielectric measurements were conducted in the frequency range of 1 to 20 MHz using an HP 4192A impedance analyzer. The dielectric constant (ε') of the pristine and sonicated P3HT samples was calculated employing the following formula:

$$\varepsilon' = C \cdot t/\varepsilon_0 \cdot A$$

Here, ε_0 represents the permittivity of free space, which has a value of 8.854×10^{-12} Farads per meter (F/m). C is the capacitance of the specimen measured during the experiments. The thickness (t) and area (A) of the specimen are measured in centimeters and square centimeters, respectively. This formula facilitates the precise calculation of the dielectric constant of P3HT based on its physical dimensions and the measured capacitance, providing insight into its dielectric properties within the specified frequency range. The structural properties of P3HT films were analyzed using a photoluminescence (PL), UV-visible optical absorption spectrometers and grazing incidence x-ray Diffraction (GIXD).

3. RESULTS AND DISCUSSION

The comparison of absorption peaks between pristine and sonicated P3HT offers valuable insights into the structural packing of the polymer chains.

The main peak in the absorption spectrum in Figure 1 is typically associated with the π-π* transition, which is sensitive to the packing and ordering of the polymer chains due to π-π stacking interactions.

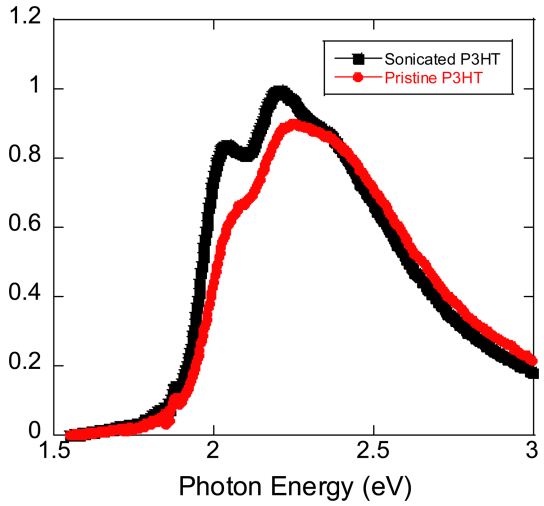

Fig. 1. Plots of optical absorbance as a function of photon energy for pristine and sonicated P3HT films.

Moreover, the observed red shift in the spectra could signify a transition from predominantly *J*-type or a less pronounced *H*-type aggregation to a more distinct *H*-type interaction. This shift suggests a change in the molecular arrangement and interaction within the P3HT structures, where the polymer chains shift from a configuration that is more aligned and linear (*J*-type) to a more face-to-face, tightly packed arrangement (*H*-type). The *H*-type interaction typically leads to a reduction in the energy gap between molecular orbitals, which is reflected in the absorption of longer wavelengths (lower energy light), thus resulting in the red shift. This transformation indicates significant changes in the electronic and optical properties of the material, which are crucial for its applications in organic electronics.

The PL spectra in Figure 2 provide insights into the electronic transitions and the nature of excitons within a material. When a conjugated polymer like P3HT undergoes a transition from *J*-type to *H*-type aggregation due to sonication, its optical properties, including luminescence, are affected significantly. In *J*-type aggregates, the excitonic transition is typically strong and results in high PL intensity. This is because the molecular orbitals of the polymer chains are aligned in such a way (face-to-face stacking) that promotes the delocalization of excitons, resulting in radiative decay and light emission.

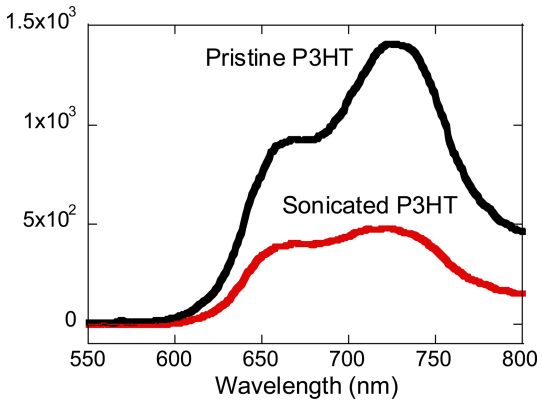

Fig. 2. Plots of PL spectra for pristine and sonicated P3HT films.

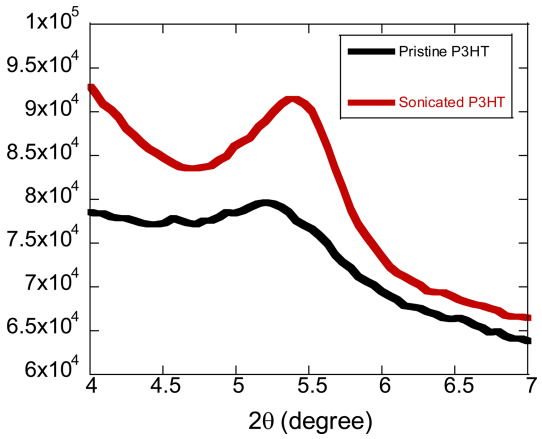

Fig. 3. Plots of GIXD for pristine and sonicated P3HT films

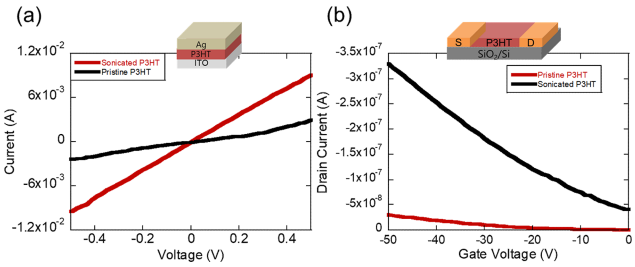

Fig. 4. Comparison of electrical properties of pristine and sonicated films using (a) a Ag/P3HT/ITP diode and (b) Au/P3HT/Au FET structures. The drain voltage was fixed at -3 V.

On the other hand, *H*-type aggregates are characterized by an edge-to-edge stacking of the polymer chains. In this configuration, the transition dipole moments of adjacent chains are in a head-to-tail arrangement, which leads to a cancellation of the transition dipole moments. As a result, the formation of *H*-aggregates typically yields non-emissive or 'dark' excitons due to the reduced overlap of π-orbitals between chains. The excitons in *H*-aggregates are less likely to decay radiatively (i.e., emit photons), leading to a lower PL intensity.

The diminished PL intensity after sonication supports the idea that sonication promotes the formation of *H*-aggregates. This formation of *H*-aggregates and the resulting non-emissive excitons are indicative of a less efficient energy transfer process for light emission. Instead of emitting photons, the energy may be dissipated through non-radiative pathways such as vibrational relaxation (phonons), intersystem crossing to triplet states, or exciton-exciton annihilation. This process, which leads to a decrease in PL intensity, confirms that the polymer chains are more tightly packed in an edge-to-edge manner post-sonication, favoring electronic interactions that do not result in luminescence.

Sonication of P3HT led to an increase in the crystallinity of the material, as evidenced by the sharper and more intense (100) peaks in the GIXD pattern in Figure 3. This result implies that the polymer chains have a more uniform and regular packing arrangement. The reduced d-spacing observed from the GIXD data indicates tighter packing of the chains, signifying stronger interchain interactions post-sonication. These stronger interactions enhance the π-π stacking within the polymer, crucial for improved electronic properties such as charge carrier mobility. The increased crystallinity, as indicated by the pronounced GIXD peaks, results from more ordered chain packing, which enhances the overall optoelectronic performance of P3HT.

The sonication-induced order-disorder transformation resulted in increased FET mobility in a lateral structure and enhanced diode performance in a vertical structure, as depicted in Figures 4(a) and 4(b). The significantly higher diode current observed in the sonicated P3HT, leading to improved conductivity (2.1×10^{-6} $\Omega^{-1}cm^{-1}$), markedly surpasses that of the pristine P3HT, which exhibited a lower conductivity of 4.0×10^{-7} $\Omega^{-1}cm^{-1}$. Figure 4(b) illustrates a comparison of FET mobility between pristine and sonicated P3HT, highlighting the increased mobility of hole carriers in the sonicated P3HT. The FET hole mobility for a sonicated P3HT film is markedly higher at 4.5×10^{-4} $cm^2\cdot V^{-1}\cdot s^{-1}$, compared to 2.6×10^{-5} $cm^2\cdot V^{-1}\cdot s^{-1}$ for a pristine P3HT film. This substantial increase in mobility is attributed to the

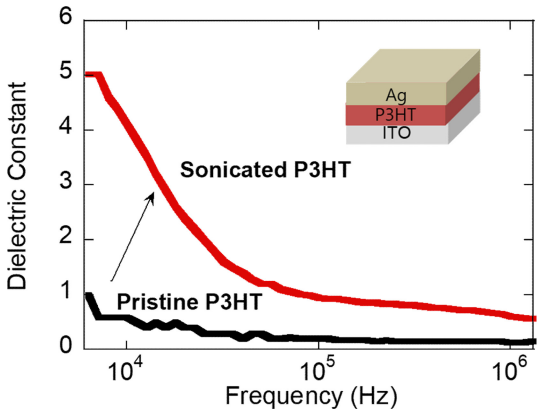

Fig. 5. Comparison of dielectric constant as a function of frequency for pristine and sonicated P3HT films.

enhanced overlap of π-orbitals, a result of the stacked lamellar structure more prominently featured in sonicated films. This conclusion is corroborated by findings from GIXD and optical absorption analyses. The reduced *d*-spacing observed from the GIXD data indicates tighter packing of the chains, signifying stronger interchain interactions post-sonication. These stronger interactions enhance the π-π stacking within the polymer, crucial for improved electronic properties such as charge carrier mobility. The increased crystallinity, as indicated by the pronounced GIXD peaks, results from more ordered chain packing, which enhances the overall optoelectronic performance of P3HT.

Importantly, we observed a large increase in the dielectric constant after sonication as shown in Figure 5. When P3HT solution is sonicated, the energy input from ultrasound can induce changes in the material's morphology and molecular ordering. This can lead to a modification of the intermolecular interactions and, consequently, a change in the dielectric properties. The increase in the dielectric constant after sonication suggests that the polymer chains have reorganized in such a way that they can better align with an applied electric field, enhancing their ability to polarize and, thus, store more electrical energy.

Figure 5 presents the frequency-dependent behavior of the dielectric constant for both pristine and sonicated P3HT films. The notable increase in the dielectric constant observed in the sonicated P3HT suggests that sonication may have induced a more homogeneous and more crystalline structure in the polymer, as corroborated by the GIXD data in Figure 3. This inference aligns with previous studies that have established a correlation between the homogeneity and crystallinity of a material and its dielectric properties. This relationship is particularly evident in the case of sonicated P3HT, where the structural modifications brought about by sonication appear to significantly influence its dielectric characteristics.

The substantial rise in the dielectric constant at low frequencies following sonication suggests a significant contribution of interface polarization to this increase. This observation indicates that the structural changes induced by sonication in P3HT notably enhance its interface polarization effects, particularly in the low-frequency region. Interface polarization, also known as Maxwell-Wagner-Sillars (MWS) polarization, occurs in materials composed of mixtures or layers with differing dielectric properties.[18] [19] When an external electric field is applied, charge carriers are impeded or accumulate at the interfaces between different materials due to the disparity in conductivities and dielectric constants. This leads to a localized build-up of charge. At low frequencies, there is enough time for charges to accumulate at the interfaces, leading to significant polarization. At high frequencies, charges do not have sufficient time to build up, and the effect diminishes. This interfacial charge accumulation enhances the overall dielectric response of the material, resulting in an increased dielectric constant, especially at lower frequencies.

In the case of P3HT, sonication could lead to a reorganization of the polymer chains, potentially creating more interfaces within the material where charges can accumulate. This can happen in several ways. Sonication might induce phase separation on a microscopic scale within the polymer, leading to regions of different crystallinity or molecular density. The interfaces between these regions can trap charges when an external electric field is applied, leading to increased polarization. On the other hand, P3HT chains may be entangled in the pristine state. Sonication could cause these chains to unfold or disentangle, leading to a more extended chain conformation and a different interface between chains. The interfaces between crystalline and amorphous regions can contribute to interface polarization. Reichmanis *et. al* reported that sonication induces a

transformation from a predominantly amorphous phase to a more complex structure with distinct ordered and disordered/quasi-ordered phases.[20] The ordered phase, characterized by nanofibrillar structures, enhances charge transport properties, while the disordered/quasi-ordered phases act as both facilitators and impediments to charge transport. Large nanofibers, formed by sonication, constitute an ordered phase. They likely consist of polymer chains in extended conjugated states, facilitating charge transport. In disordered/quasi-ordered regions, polymer chains have a twisted and disordered conformation. They act as charge transport conduits between the ordered domains but are also bottlenecks for charge transport. Our GIXD findings, corroborated by absorption and PL results, indicate that the enhanced crystallinity in thin films directly results from an increased distribution of microcrystallites throughout the films. This observation supports the hypothesis that sonication leads to the formation of distinct ordered regions interspersed within disordered or quasi-ordered areas. The enhancement in the dielectric constant, driven by interface polarization, highlights the significant influence of sonication on the microstructure of P3HT. Sonication likely induces the formation of new interfaces, especially between ordered and disordered or quasi-ordered regions, facilitating charge accumulation at these junctions. This alteration in microstructure, a consequence of sonication, correlates with the observed rise in the dielectric constant, indicative of an improved ability for polarization under the influence of an electric field.

Our research demonstrates that sonication led to a significant change in the dielectric properties of P3HT. Specifically, there is an observable transition from less prominent *H*-type to *H*-type aggregation, which has profound effects on the material's electronic structure and optoelectronic performance. This transition was confirmed through changes in the absorption and PL spectra, indicating a more localized electronic character and the formation of non-emissive excitons in the case of *H*-aggregates. Additionally, the study explores the concept of interface polarization, especially the Maxwell-Wagner-Sillars polarization, which could explain the observed increase in the dielectric constant following sonication. This effect is likely due to the creation of new interfaces within the P3HT material where charges can accumulate, as supported by various experimental observations and analyses. Our findings highlight the potential of using sonication as a technique for tuning the dielectric properties of P3HT and possibly other conjugated polymers. This has significant implications for optimizing the materials for use in organic electronics. The research contributes to the broader understanding of polymer physics and the development of organic electronic devices by showing how the manipulation of microstructural environments can control material properties.

ACKNOWLEDGEMENT

This research was supported by the Basic Science Research Program through the National Research Foundation of Korea (NRF) funded by the Ministry of Education (NRF-2015R1A6A1A03031833, NRF-2019R1F1A1060042 and NRF-2020R1A2C1007258). This work was also supported by the 2024 Hongik Faculty Research Support Fund.

REFERENCES

1. Peters, V. N. Tumkur, T. U. Zhu, G. Noginov, M. A., Sci Rep **5**, 14620 (2015).
2. Handloser, M. Dunbar, R. B. Wisnet, A. Altpeter, P. Scheu, C. Schmidt-Mende, L. Hartschuh, A., Nanotechnology **23**, 305402 (2012).
3. Hou, S. Yu, J. Zhuang, X. Li, D. Liu, Y. Gao, Z. Sun, T. Wang, F. Yu, X., ACS Appl Mater Interfaces **11**, 44521 (2019).
4. Panahandeh-Fard, M. Yin, J. Kurniawan, M. Wang, Z. Leung, G. Sum, T. C. Soci, C., J Phys Chem Lett **5**, 1144 (2014).
5. Wang, C. H. Chen, C. W. Chen, Y. T. Chen, C. T. Chen, Y. F. Chou, S. W. Chen, C. C., Nanotechnology **22**, 065202 (2011).
6. Hynynen, J. Kiefer, D. Muller, C., RSC Adv **8**, 1593 (2018).
7. Yin, W. Dadmun, M., ACS nano **5**, 4756 (2011).
8. Ferreira, B. da Silva, P. F. Seixas de Melo, J. S. Pina, J. Macanita, A., J Phys Chem B **116**, 2347 (2012).
9. Thomas, A. K. Garcia, J. A. Ulibarri-Sanchez, J. Gao, J. Grey, J. K., ACS nano **8**, 10559 (2014).
10. Eder, T. Stangl, T. Gmelch, M. Remmerssen, K. Laux, D. Höger, S. Lupton, J. M. Vogelsang, J., Nature communications **8**, 1641 (2017).

11. Boehm, B. J. McNeill, C. R. Huang, D. M., Nanoscale **14**, 18070 (2022).
12. Liu, H. Xu, J. Li, Y., Acc Chem Res **43**, 1496 (2010).
13. Spano, F. C. Silva, C., Annual Review of Physical Chemistry **65**, 477 (2014).
14. Ehrenreich, P. Birkhold, S. T. Zimmermann, E. Hu, H. Kim, K. D. Weickert, J. Pfadler, T. Schmidt-Mende, L., Sci Rep **6**, 32434 (2016).
15. Alam, K. M. Garcia, J. C. Kiriakou, M. V. Chaulagain, N. Vrushabendrakumar, D. Cranston, E. D. Gusarov, S. Kobryn, A. E. Shankar, K., Nanotechnology **34**, 205703 (2023).
16. Martin, T. P. Wise, A. J. Busby, E. Gao, J. Roehling, J. D. Ford, M. J. Larsen, D. S. Moule, A. J. Grey, J. K., J Phys Chem B **117**, 4478 (2013).
17. Dou, F. Li, J. Men, H. Zhang, X., Polymers (Basel) **12**, 786 (2020).
18. Samet, M. Kallel, A. Serghei, A., Journal of Composite Materials 56, 3197 (2022).
19. Starczewska, A. Mistewicz, K. Kozioł, M. Zubko, M. Stróż, D. Dec, J., Materials **15**, 1543 (2022).
20. Aiyar, A. R. Hong, J. I. Nambiar, R. Collard, D. M. Reichmanis, E., Advanced Functional Materials **21**, 2652 (2011).